OPHELIA 58 (3): 135-150 (December 2004)

PART 1:
Microbial mats exposed or not to oil pollution

OIL-CONTAMINATION EFFECTS ON A HYPERSALINE MICROBIAL MAT COMMUNITY (CAMARGUE, FRANCE) AS STUDIED WITH MICROSENSORS AND GEOCHEMICAL ANALYSIS

Mikkel Benthien[1], Andrea Wieland[1,], Tirso García de Oteyza[2], Joan O. Grimalt[2] and Michael Kühl[1]*

[1]Marine Biological Laboratory, Institute of Biology,
University of Copenhagen, Strandpromenaden 5, DK-3000 Helsingør, Denmark

[2]Department of Environmental Chemistry (ICER-CSIC),
Jordi Girona 18, E-08034 Barcelona, Spain

*Corresponding author: wieland@geowiss.uni-hamburg.de, present address: Institute for Biogeochemistry and Marine chemistry, University of Hamburg, Bundesstr. 55, D - 20149 Hamburg, Germany

ABSTRACT

Pristine microbial mat samples from a hypersaline pond of a solar saltern (Camargue, France) were transferred into microcosms, contaminated in the laboratory with a viscous sulphur-rich crude oil, and characterized over time with microsensors for O_2, pH and H_2S, respectively. The goal was to gain information on how oil pollution affects the major autotrophic and heterotrophic processes involved in carbon cycling in coastal mats. Further, GC-MS analysis of mat samples taken directly after microsensor measurements was performed to investigate how the composition and the amount of oil changed over time in the oil contaminated mats. Pronounced biogeochemical changes in the microbial mat samples were observed during the experiment. The obtained results indicate that oil contamination stimulated organotrophic aerobic respiration and that C21-C28 alkanes of the crude oil were degraded/oxidized over time within the contaminated mats.

INTRODUCTION

Microbial mats are cohesive and stratified microbial communities growing on solid surfaces. In coastal areas such mats are known to stabilize sediments. Perennial and thick microbial mats thrive under extreme enviromental conditions e.g. habitats with elevated salinity (Cohen 1989, Javor 1989) that exclude or limit the survival of higher organisms but prolific mat growth can also be induced in normal defaunated sediment (Kühl et al. 2003). In many microbial mats cyanobacteria are the principal primary producers of organic matter and oxygen. Because of a very close coupling between autotrophic and heterotrophic processes in microbial mats, most of the organic matter produced by the cyanobacteria is recycled within the uppermost active zone. Sulphate reduction is considered to be the most important anaerobic mineralisation process in cyanobacterial mats (Jørgensen et al. 1992, Canfield & Des Marais 1993, Wieland et al. 2004). The sulphide produced by the sulphate-reducing bacteria can be oxidized abiotically in the oxic zone but is primarily depleted by chemotrophic colourless sulphur bacteria and anoxygenic phototrophs, which are both located around the oxic-anoxic interface in the mat.

The continuing demand for oil has led to a high frequency of transportation of oil, thereby increasing the risk of detrimental oil spills in coastal environments. Crude oil is a mixture of hydrocarbon compounds of biogenic origin that occur naturally in the earth (Fingas 2001). The hydrocarbons in oils are divided into three major groups: saturated (alkanes, cyclo-alkanes and waxes), aromatic (e.g benzene, toluene, xylenes), and polar compounds (resins and asphaltenes). Of these, the first two groups include compounds, which are readily oxidized under aerobic conditions by a wide variety of

microorganisms like *Bacillus* spp. and *Pseudomonas* spp., whereas resins and asphaltenes are more recalcitrant to microbial degradation (Fingas 2001). Some crude oil components can under optimal environmental conditions serve as carbon sources for microorganisms, as described for *Pseudomonas* spp. and *Rhodococcus* spp. Sub-optimal conditions result in only partial oxidation of these compounds. The intermediates, e.g., alcohols and fatty acids, can again serve as carbon sources for other microorganisms, which cannot attack the oil components directly, like, e.g., anaerobic sulphate-reducing bacteria (Bertrand et al. 1989).

Under controlled conditions, bioremediation based on the use of microorganisms is a practical and cost-effective method to remove pollutants such as hydrocarbons from contaminated surfaces and sub-surfaces (e.g., Holliger et al. 1997, Obuekwe & Al-Zarban 1998) but the microorganisms must be present in sufficient quantities and diversity in order to accomplish this. Due to the high density of diverse microbial populations and the presence of multiple and fluctuating microenviromental gradients, microbial mats have a potential to immobilize and degrade pollutants (Cohen 2002). This potential may give microbial mats an important role in many forms of bioremediation. Constructed wetlands with aquatic plants and associated microbial mats have e.g. been used for treatment of agricultural, municipal, and industrial waste (e.g. Kivaisi 2001, Mashauri et al. 2000, Shutes et al. 1999). Moreover, recent studies have shown that after the Gulf War in 1991, where 800.000 tons of oil were spilled, the development and survival of microbial mats in polluted coastal areas of the Persian Gulf played a significant role in the bioremediation of these areas (Fingas 2001, Hoffmann 1996, Sorkhoh et al. 1992).

Cyanobacterial mats appear to thrive even when subjected to severe oil pollution. Although such mat systems are likely to be of increasing importance for bioremediation of oil pollution in environmentally sensitive ecosystems, yet very little information on the biogeochemistry of mats polluted with crude oil is currently available. Recently, the effect of selected clay-immobilized model compounds (phenanthrene, pristane, octadecane, and dibenzothiophene) on the structure and function of pristine hypersaline mats was described (Grötschel et al. 2002). This laboratory study showed that despite decreasing concentrations of petroleum model compounds in the mat, neither metabolic changes nor shifts in the microbial community were observed.

In our study, pristine hypersaline microbial mats from a solar saltern (Salin-de-Giraud, Camargue, France) (Cornée et al. 1992, Wieland et al. 2004, Fourçans et al. 2004) were transferred into microcosms, contaminated in the laboratory with crude oil and characterized over time with microsensors for O_2, pH, and H_2S, respectively. In parallel to this, mat subsamples were frozen directly after microsensor measurements for chemical analyses to determine the degree of contamination and hydrocarbon degradation in the mat community over time. The goal was to gain detailed information on how oil contamination affects the major autotrophic and heterotrophic processes involved in carbon cycling in pristine hypersaline mats.

RESULTS

Mat structure

The microbial mats were very cohesive with a smooth green surface layer, dominated by the filamentous cyanobacterium *Microcoleus chthonoplastes*. The detailed microbial composition of the mat community was described by Fourçans et al. (2004), showing that besides different cyanobacteria, also diatoms, sulphate-reducing bacteria, sulphur-oxidizing and anoxygenic phototrophic bacteria were present in the mat. An intense black color of deeper layers in the mat indicated high sulphate reduction rates and high iron concentrations (Wieland et al. 2004).

After contamination, the crude oil on the mat surface disappeared within a few days. However, miniature oil droplets continued to be released from the upper mat layers when samples were cut throughout the experiment, showing that the oil had penetrated and was incorporated into the mat fabric (Fig.1). A macroscopic change of the mat surface was observed in the contaminated mats. The original green color of the mat surface changed to brownish-orange and the surface topography became very heterogeneous with a gelatinous top layer of exopolymers formed by the mats (Fig. 1). The increased surface roughness resulted in an increasing thickness of the effective diffusive boundary layer, δ_e (Table 1).

Microprofiles of O_2 and gross photosynthesis

In Figure 2, examples of steady-state O_2 profiles in darkness and light (348 µmol photons m^{-2}

Table 1: Oxygen penetration, maximal O_2 concentration, the thickness of the photic zone, areal rates of gross photosynthesis, the thickness of the effective DBL, and maximal volumetric gross photosynthesis rates as a function of time in the different mats.

Control

Day	O_2 penetration	Maximal O_2 concentration	Photic zone	Gross photosynthesis	Maximal gross photosynthesis	Thickness of effective DBL
	(mm)	(μM)	(mm)	(nmol O_2 cm^{-2} s^{-1})	(nmol O_2 cm^{-3} s^{-1})	(μm)
-8	1.5	1460	1	0.66 ± 0.28	16.1	278
0	1.05	1420	0.8	0.73 ± 0.08	15.5	239
6	1.65	1283	1.05	0.76 ± 0.10	18.3	269
13	1.55	1130	1.1	0.59 ± 0.04	8.6	313
26	2.3	1060	1.3	0.82 ± 0.08	13.2	550
98	2.25	847	0.95	0.32 ± 0.08	5.1	479

Light contamination

Day	O_2 penetration	Maximal O_2 concentration	Photic zone	Gross photosynthesis	Maximal gross photosynthesis	Thickness of effective DBL
	(mm)	(μM)	(mm)	(nmol O_2 cm^{-2} s^{-1})	(nmol O_2 cm^{-3} s^{-1})	(μm)
-8	1.5	1460	1	0.66 ± 0.28	16.1	278
0	1.85	1412	1.5	0.83 ± 0.07	16.3	244
6	1.4	855	1.1	0.92 ± 0.03	11.1	226
13	1.2	1100	0.7	0.45	11.1	252
26	1.95	1159	1.3	0.51 ± 0.07	7.6	291
98	1.6	1021	1	0.43 ± 0.04	10.1	488

Heavy contamination

Day	O_2 penetration	Maximal O_2 concentration	Photic zone	Gross photosynthesis	Maximal gross photosynthesis	Thickness of effective DBL
	(mm)	(μM)	(mm)	(nmol O_2 cm^{-2} s^{-1})	(nmol O_2 cm^{-3} s^{-1})	(μm)
-8	1.5	1460	1	0.66 ± 0.28	16.1	278
0	1.05	980	0.7	0.59	13.1	291
6	1.35	1243	1	0.85	12.7	196
13	1.65	1300	0.9	0.58 ± 0.02	12.5	341
26	1.55	962	0.9	0.23 ± 0.06	3.5	415
98	1.05	944	0.7	0.6 ± 0.3	10.9	361

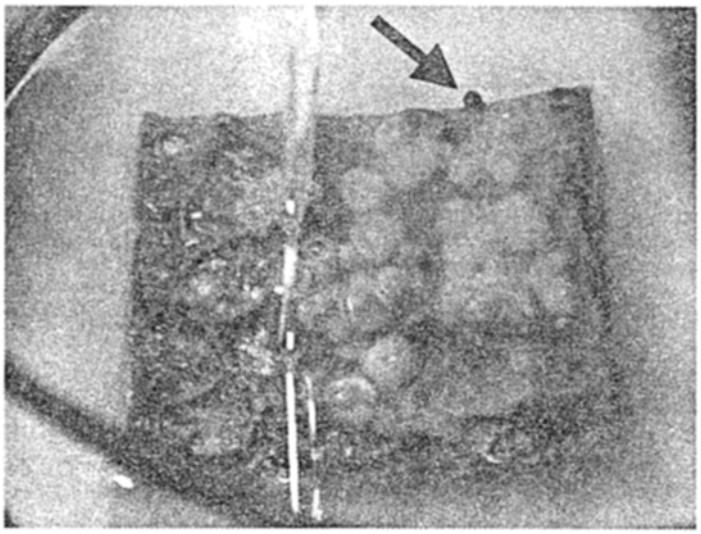

Fig. 1. Oil-contaminated microbial mat with a brownish-orange gelatinous top layer of exopolymers. Note the miniature oil droplet released from the mat, as indicated by the arrow.

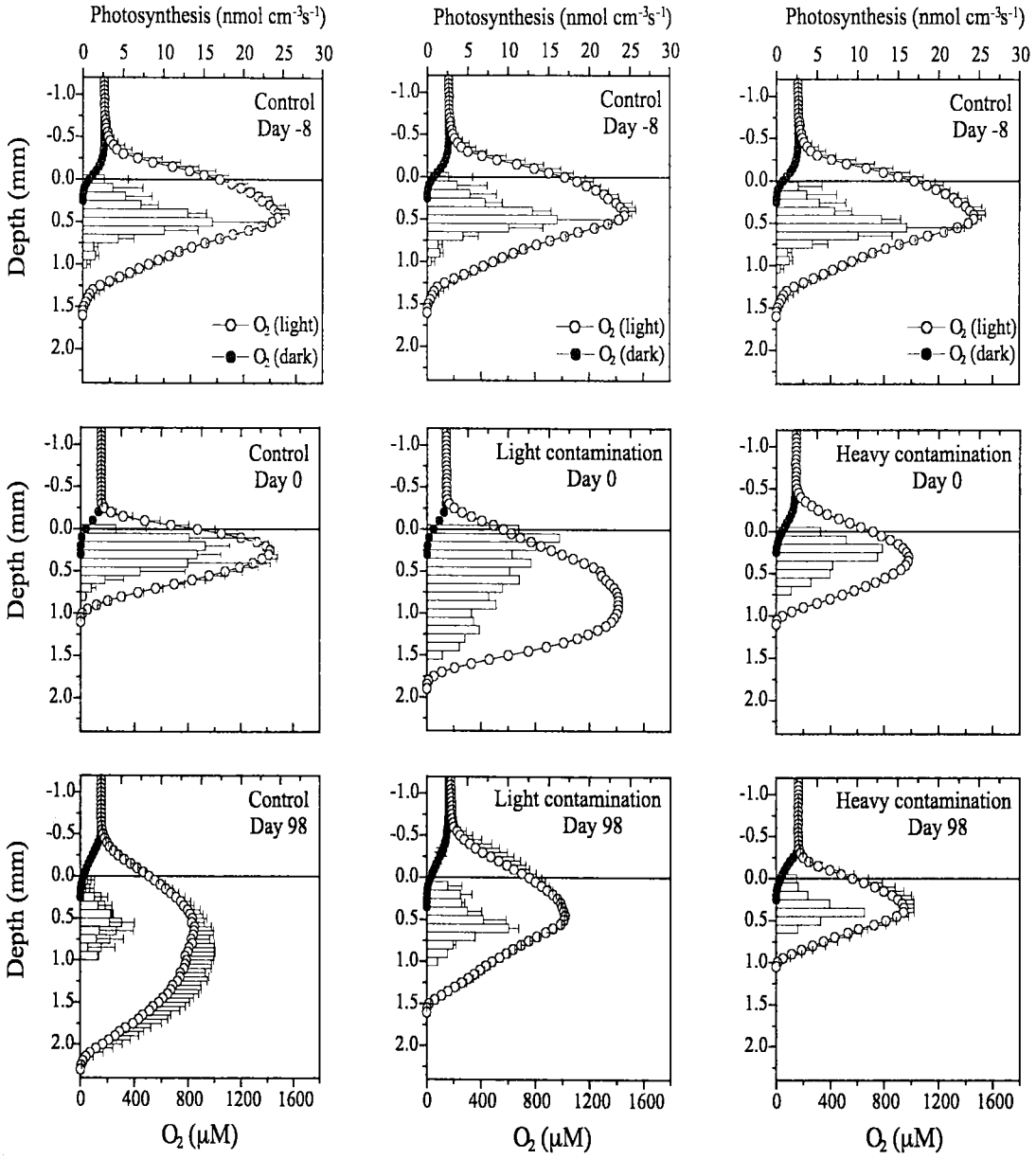

Fig. 2. Examples of average steady-state concentration profiles of O_2 in the control mat, light contaminated and heavily contaminated mat as a function of time after contamination. Bars represent average rates of volumetric gross photosynthesis. Standard deviation is indicated by error bars (n = 2-5). Dark symbols show profiles in the dark incubated mat, open symbols in the illuminated mat (348 μmol photons m^{-2} s^{-1}).

s^{-1}) are shown in the 3 differently treated mats as a function of time after contamination. Dark O_2 profiles were generally not affected by contamination with crude oil. Maximal O_2 levels in the illuminated mats were highest in the beginning of the experiment and showed a decreasing trend with increasing incubation time in all three mats (see also Table 1). In the control mat, O_2 penetration depth showed an increasing trend with incubation time, whereas the opposite effect was observed in the heavily contaminated mat. At the end of the experiment,

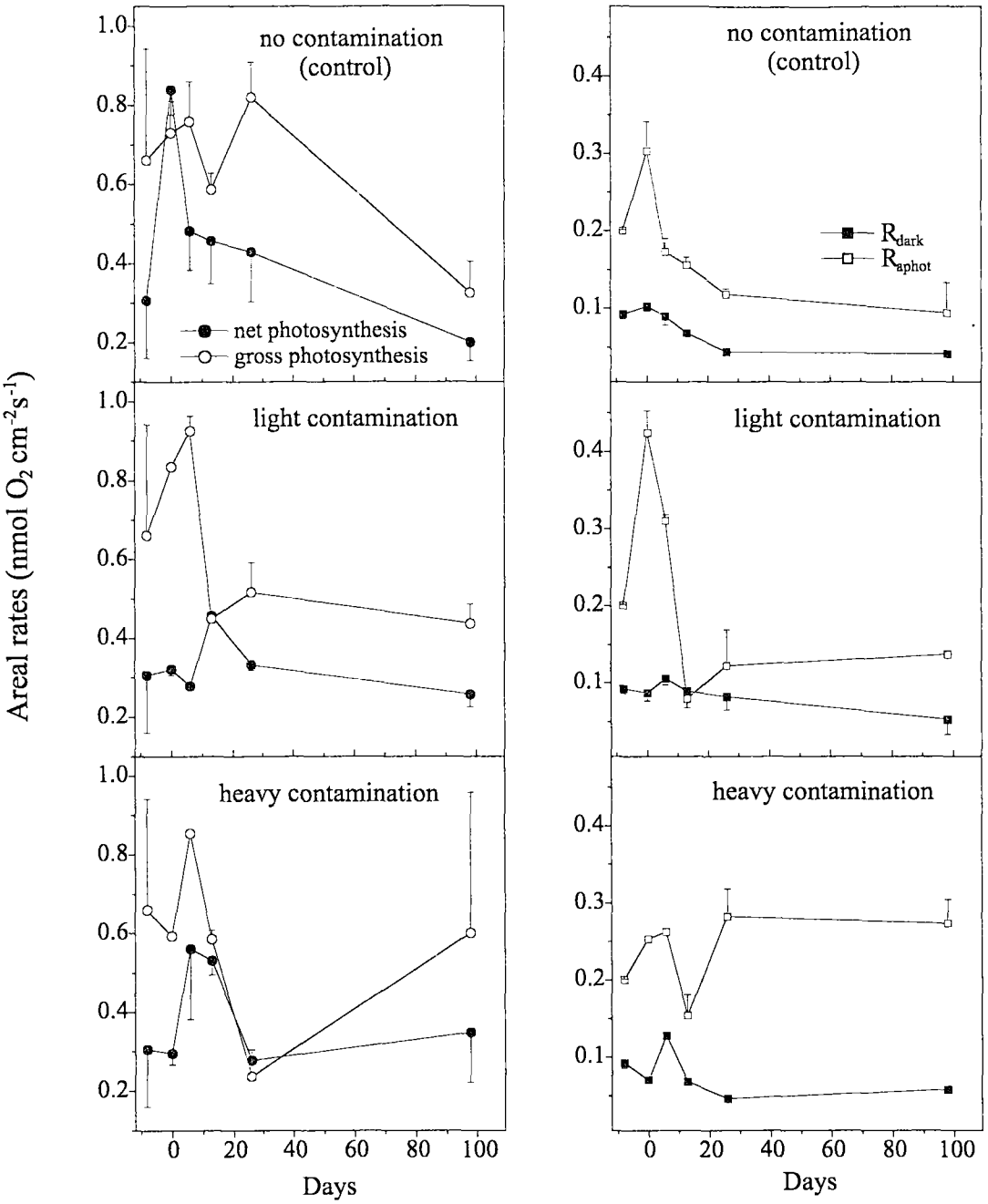

Fig. 3. Areal rates (mean ± standard deviation) of net and gross photosynthesis (left panel), and of dark O_2 consumption (R_{dark}) and O_2 consumption in the aphotic zone, R_{aphot} (right panel), as a function of time in the mats.

the thickness of the oxic zone in which no photosynthetic activity was detectable, i.e., the aphotic oxic zone, showed a decreasing trend as a function of oil contamination (Fig. 2, lower panel). The photic zone was ~1 mm deep in all three mats. The maximal volumetric gross photosynthesis rate showed a decreasing trend with incubation time, with the decrease being most pronounced in the control mat (Fig. 2, Table 1).

Oxygen conversion rates

In the uncontaminated mat, gross photosynthesis rates showed an increasing trend during the first 26 days and a pronounced decrease with increasing time (Fig. 3, upper panel). After an initial increase, net photosynthesis rates decreased constantly with time. At day 0, net photosynthesis rates were higher than gross photosynthesis rates, a phenomenon previously observed in cyanobacterial mats (Epping & Kühl 2000, Wieland & Kühl 2000b) and ascribed to light-dependent oxygen consumption associated with Mehler reactions. Oxygen consumption rates in the aphotic oxic zone, R_{aphot}, determined as the downward O_2 flux into the mat (J_s), showed an initial increasing trend, but started to decrease after day 6. Dark O_2 consumption rates, R_{dark}, were relatively stable in the beginning, but decreased to approximately half the rate at day 26.

Gross photosynthesis in the light contaminated mat initially increased and then stabilized with a decreasing trend over time (Fig. 3, middle panel). Net photosynthesis rates were relatively stable throughout most of the experiment. The R_{aphot} showed the same trend as in the uncontaminated mat, but the effect was more pronounced. In the beginning, R_{aphot} increased strongly to more than double the initial rate, after which it strongly decreased and then stabilized. The R_{dark} was more or less stable over time, with a slight decrease 98 days after contamination.

In the heavily contaminated mat, gross and net photosynthesis rates showed more or less the same trends (Fig 3, lower panel). The R_{dark} initially increased after contamination and then decreased again to a relative stable, but lower rate. The R_{aphot} was more or less stable over time after an initial increase, and remained at a ~2-2.5 times higher level than in the control mat.

Figure 4 shows the areal O_2 conversion rates of the light and heavily contaminated mats expressed relative to the rates in the uncontaminated mat. The relative gross and net photosynthesis rates (left panel) had more or less the same trend in both mats. After an initial period of slight increases and decreases, the contaminated mats showed at day 98 a higher O_2 production (net and gross photosynthesis) than the uncontaminated mat. The heavily contaminated mat showed the most pronounced increase, resulting in a gross photosynthesis rate almost 90% higher than the control mat. Re lative dark O_2 consumption rates (upper right panel) and R_{aphot} (lower right panel) increased over time, with a strong increase of R_{aphot} in the heavily contaminated mat, resulting in almost 200% higher rates as compared to the control mat. Thus, oil contamination clearly led to an increase of O_2 consumption in the mats.

Microprofiles of pH, H_2S, and S_{tot}

Examples of dark steady-state pH, H_2S, and total sulphide (S_{tot}) profiles in the uncontaminated and heavily contaminated mat are shown in Fig. 5 as a function of time after contamination. In the beginning of the experiment, the pH in both mats dropped from a value of 8.2 in the water to pH 7.1 at 2.5-3 mm depth. After 98 days, the pH decreased more strongly in the uppermost layer of both mats leading to a pH drop from a value of 8.2 in the water to pH 7 already at 0.7-1 mm depth. In the uncontaminated and heavily contaminated dark incubated mats, H_2S and S_{tot} levels were highest in the beginning of the experiment (day 0) and decreased towards the end of the experiment (middle and right panel). In the uncontaminated mat, maximal concentrations of 648 μM S_{tot}, corresponding to 290 μM H_2S at the prevailing pH of 7.1 at 3.1 mm depth, decreased to 138 μM S_{tot} and 81 μM H_2S at pH 6.9 at the same depth (day 98). Compared to the uncontaminated mat, sulphide levels decreased stronger directly after contamination of the heavily contaminated mat, but the sulphide level in the latter was slightly higher 98 days after contamination.

In Figure 6, examples are shown of steady-state pH, H_2S, and S_{tot} profiles in the illuminated uncontaminated and heavily contaminated mats as a function of time after contamination. Photosynthetic CO_2 fixation in the mats led to a maximum of pH (up to pH 9.4-9.5) at ~0.5 mm depth, indicating high photosynthesis rates in this layer (Fig. 6, left panel). Below this peak, pH strongly decreased due to aerobic respiration, fermentation, and sulphide oxidation. Directly after oil contamination (day 0), this pH peak decreased in the heavily contaminated mat to pH 8.7 at 1.3 mm depth. At the end of the experiment (day 98), the pH maximum in the uppermost layer of the uncontaminated mat was very broad with pH ~9.7 at 0.3-1.5 mm depth.

At day 0, the sulphide levels in the illuminated mats increased, but decreased again at the end of the experiment. In the uncontaminated mat, maximal concentrations of 401 μM

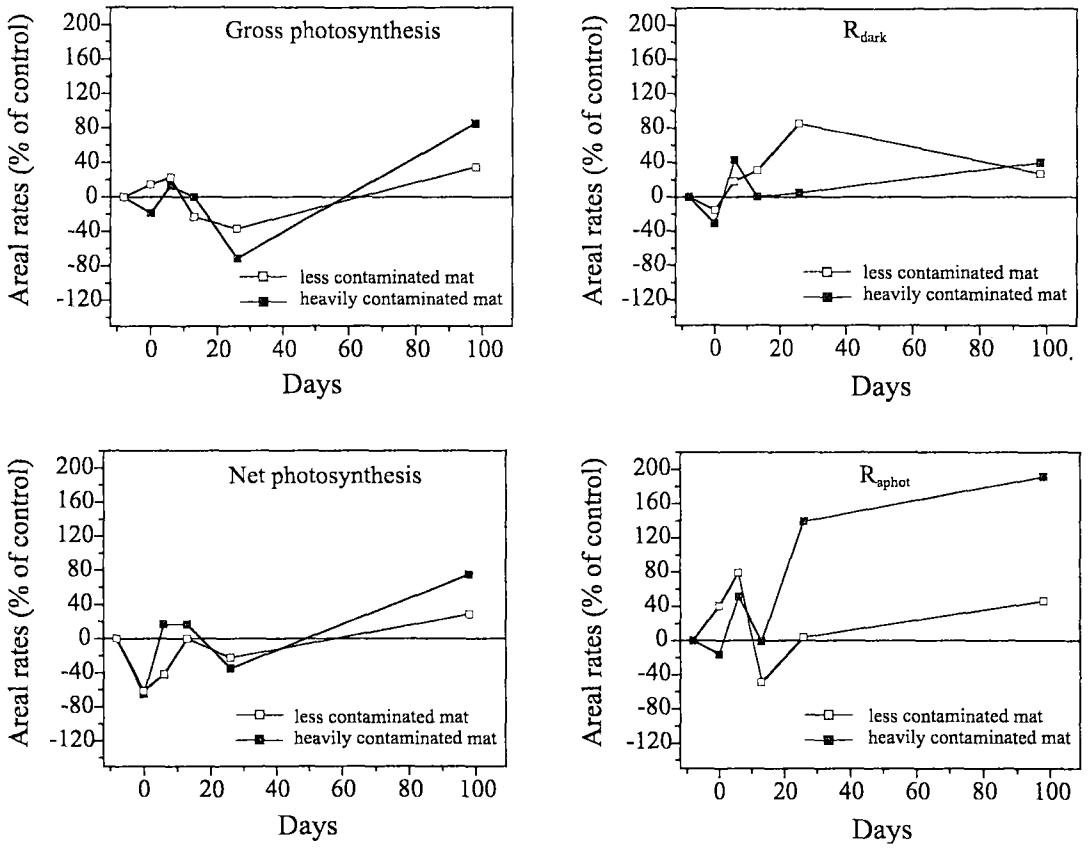

Fig. 4. Areal rates of net and gross photosynthesis (left panel), and of dark O_2 consumption, R_{dark}, and O_2 consumption in the aphotic zone, R_{aphot} (right panel), in the light and heavily contaminated mats expressed relative to the rates in the uncontaminated mat.

of total sulfide, corresponding to 272 μM H_2S at the prevailing pH of 6.6 at 3.5 mm depth, was found at day 0. At the end of the experiment (day 98), S_{tot} and H_2S decreased in the uncontaminated mat to 257 and 88 μM (pH 7.3) at 3.5 mm depth, respectively. Compared to the uncontaminated mat, sulphide levels decreased more strongly directly after contamination in the heavily contaminated mat than in the control, but the sulphide levels were more or less the same at the end of the experiment (day 98). Thus, the sulphide profiles did not show strong changes in response to oil contamination and exhibited a similar decreasing trend during the experiment.

Crude oil compounds in the mat

To determine the amount and fate of crude oil in the mats, extracts of the uppermost mat layer (0.1-0.3 cm) were analysed by gas chromatography. The *n*-alkanes originating from the crude oil were identified, traced over time, and quantified in relation to a microbial mat lipid, *n*-triacos-1-ene. We found a gradual depletion of *n*-alkanes in the mat immediately after oil pollution (Fig. 7). Quantification was only performed from the C_{21} alkane onwards, as the unpolluted microbial mat itself contained some of the lighter *n*-alkanes. Also, the depletion of *n*-alkanes lighter than C_{18} is due to e.g. evaporation, and their disappearance does not imply biodegradation (Kuo 1994). In the heavily contaminated mats, C_{21}-C_{28} alkanes decreased strongly in the mat and were virtually absent at the end of the experiment (Fig. 8), indicating degradation and/or transformation of these compounds within the microbial mat. The decrease of the *n*-alkanes was highest during the first 26 days after contamination.

DISCUSSION

Our results showed that the sulphur-rich crude oil was degraded over time, leading to an increased O_2 consumption in the contaminated mats relative to the uncontaminated control mats.

Photosynthesis and O_2 consumption in the uncontaminated mat

The mat surface changed over time from a relative smooth surface to a very heterogeneous surface topography (Fig. 1), increasing effective diffusive boundary layer thickness, δ_e (Table 1; Jørgensen 2001). Dark O_2 consumption rates, R_{dark}, in the microbial mats were limited by the diffusive O_2 supply over the diffusive boundary layer (DBL) (Jørgensen 1994, Jørgensen 2001, Jørgensen & Des Marais 1990, Kühl & Jørgensen 1992). Thus, the observed decrease of R_{dark} over time (Fig. 3) can partly be explained by a reduced O_2 supply due to a thicker DBL.

After the mats had been introduced into the microcosms, increased photosynthesis rates were observed (day -8 to 26, Fig. 3), but photosynthesis rates and O_2 concentration in the uncontaminated mat decreased in general during the experiment (Fig. 3, Table 1). Furthermore, both R_{dark} and R_{aphot} decreased strongly over time (Fig. 3), suggesting a decrease of sulphide oxidation and/or organotrophic O_2 respiration in the mat, which determine both rates. A decrease of heterotrophic activity can reduce the internal CO_2 supply for photosynthesis in the mat, leading to declining productivity with time. Indeed, data showed decreasing H_2S and sulphide (S_{tot}) concentrations with time in both the illuminated and dark incubated control mat (Figs. 5, 6). We speculate that decreasing rates of oxygen and sulphide turnover in the control mat were caused by an increasing limitation of organic substrate or inorganic nutrients in the mat.

Photosynthesis and O_2 consumption in the contaminated mat

In the heavily contaminated mat, a decrease of O_2 levels and O_2 penetration depth was observed over time (Fig. 2, Table 1). R_{aphot} and R_{dark} increased strongly and were 200 and 40% higher, respectively than the rates in the uncontaminated mat at the end of the experiment (Fig. 4). This suggests that the oil contamination stimulated O_2-consuming processes, especially over longer time periods.

Compared to the control mat, the sulphide levels decreased stronger in the heavily contaminated mat directly after contamination, but were slightly higher 98 days after contamination (Fig. 5). Thus, changes in O_2 consumption were most probably not caused by increased sulphide oxidation, pointing to an increase of heterotrophic aerobic respiration in the oil-contaminated mats.

At the end of the experiment, higher net and gross photosynthesis rates were detected in the two contaminated mats as compared to the uncontaminated mat. This could be a result of an increased availability of CO_2 due to the stimulation of aerobic heterotrophic respiration. It has been shown previously that photosynthesis and respiration are closely coupled in microbial mats, and that the dissolved inorganic carbon requirement of the photosynthetic population may largely be covered by the respiration of closely associated heterotrophs (Canfield & Des Marais 1993, Glud et al. 1992, Kühl et al. 1996, Wieland & Kühl 2000a).

Despite the general increasing trend of photosynthesis rates, a significant decrease of gross photosynthesis rates was observed shortly after the contamination (Figs. 3, 4). After day 13, gross photosynthesis rates in the less contaminated mat stabilized, whereas the rates in the heavily contaminated mat continued to decrease until day 26. The amount of oil added onto the mat apparently affected gross photosynthetic activity. It is well known that crude oils contain compounds, which are inhibitory for photosynthetic organisms even at very low concentrations (Narro 1987). Light limitation caused by the layer of crude oil on top of the mat could also have led to the temporary decrease of gross photosynthesis. Degradation of the hydrocarbons and possibly also diffusion of water-soluble compounds out of the mat could have led to the recovery of gross photosynthesis rates at the end of the experiment (Figs. 3, 4). Chemical analyses of the oil contaminated mat samples showed that most of the *n*-alkanes originating from the crude oil had disappeared almost completely after day 26 (Figs. 7, 8).

Sulphide cycling in the mats

Profiles showed that sulphide levels and net sulphide turnover rates decreased strongly over time in both the uncontaminated and heavily contaminated mats, especially during dark incubations (Figs. 5, 6). In the illuminated mats, total sulphide concentrations in both the

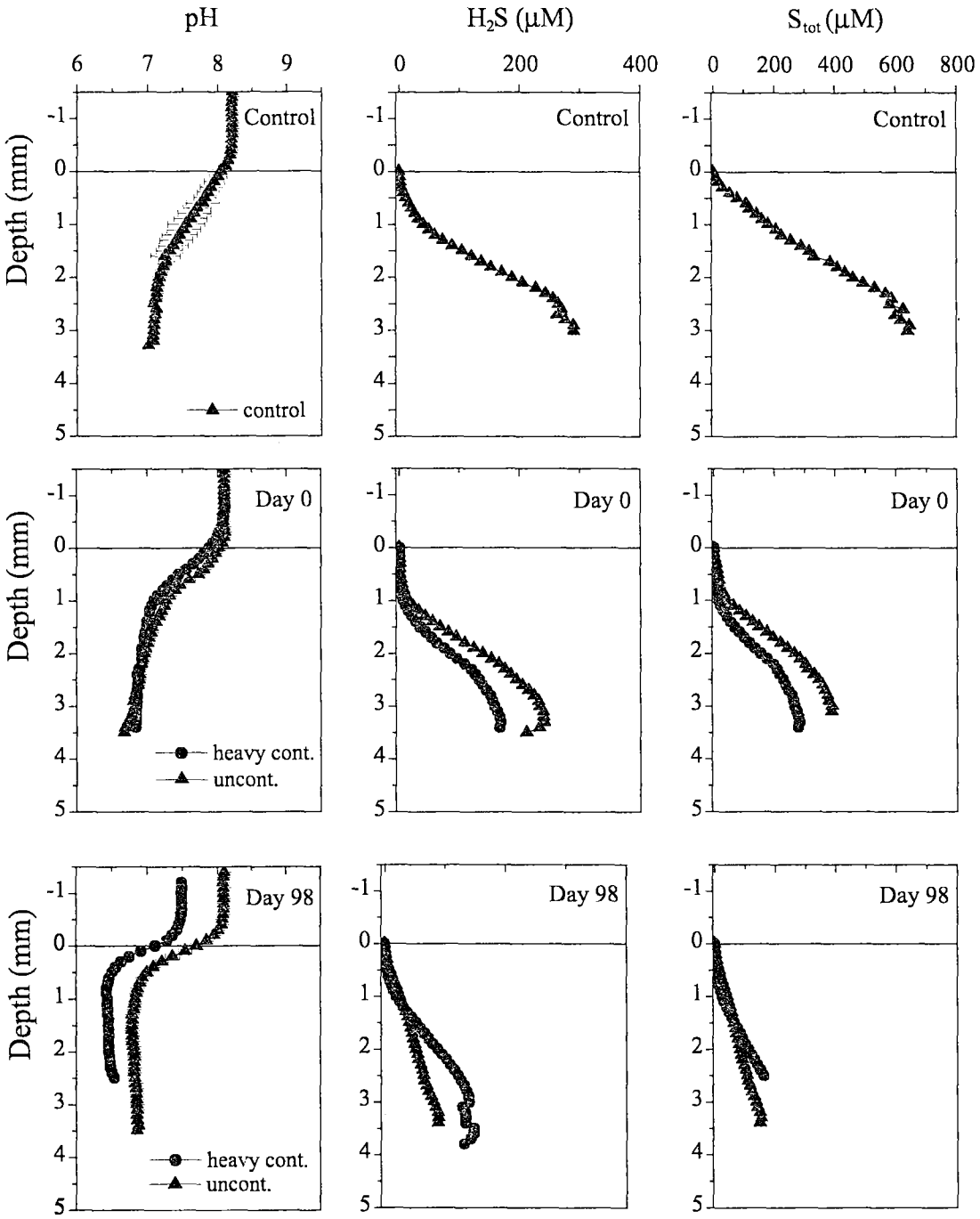

Fig. 5. Average steady-state concentration profiles (n = 2-3) of pH, H_2S, and total sulphide (S_{tot}) as a function of time in the dark incubated mats.

uncontaminated and the heavily contaminated mats increased slightly in the beginning of the experiment, but remained more or less the same over time (Fig. 6, right panel). However, sulphide turnover rates as estimated from microsensor data, underestimate sulphur cycling, especially in the Camargue mats (see Wieland et al. 2004). Biogeochemical measure-

ments performed in mats from the same location by Wieland et al. (2004) showed that high iron concentrations in the mats led to pronounced sulphide precipitation by iron, especially in anoxic mat layers. This study also showed that besides sulphide precipitation with Fe(II), also sulphide oxidation by anoxygenic photosynthesis and by Fe(III)-oxides strongly reduced the free sulphide pool despite very high sulphate reduction rates found in these mats. Thus, in the iron-rich Camargue mat, sulphide microsensor data strongly underestimate sulphur cycling and minor changes of the sulphur cycle are probably not detectable with microsensors due to the high buffering capacity of the iron. The decreasing sulphide concentrations, however, point to a decreasing sulphate-reducing activity in the mat over time, indicating that oil degradation products did not serve as (additional) substrate for sulphate reduction in the mat.

Oil degradation

Microbial degradation of oil released into the aquatic enviroment has been shown to occur by attack on the saturated hydrocarbons and low molecular weight aromatic fractions of the oil. The *n*-alkanes are considered the most readily degraded compounds in oil (Davies & Hughes 1968 and Kator et al. 1971 in Atlas & Bartha 1992). Chemical analyses of the contaminated mat samples revealed that most of the *n*-alkanes from the crude oil were degraded by the end of the experiment (Figs. 7, 8). Further, our O_2 data showed that the crude oil addition stimulated the overall activity in the contaminated mats as compared to the control. We speculate that the crude oil acted as substrate for hydrocarbon-degrading microorganisms within the mats, leading to degradation of the hydrocarbons over time.

The observed increase of O_2 consumption in the contaminated mats suggests that oil-contamination mainly stimulated aerobic heterotrophic bacteria. However, we cannot conclude whether the aerobic heterotrophs were the only organisms degrading the oil. The most prevalent genera of hydrocarbon-degrading microorganisms in aquatic environments are *Pseudomonas* sp., *Achromobacter* sp., *Arthrobacter* sp., *Micrococcus* sp., *Nocardia* sp., *Vibrio* sp., *Acinetobacter* sp., *Brevibacterium* sp., *Rhodococcus* sp., *Corynebacterium* sp., *Flavobacterium* sp., *Candida* sp., *Rhodotorula* sp. and *Sporobolomyces* sp. (Bartha and Atlas 1977). Other studies indicate that some strains of cyanobacteria are capable of oxidizing oil compounds, but evidence for this is still tentative (Ellis 1977, Al Hasan et al. 1994, Cerniglia et al. 1980). The fact that the cyanobacteria in mats are associated with hydrocarbon-degrading bacteria and fungi located in the cyanobacterial polysaccharide layers (Sorkhoh et al. 1992, García de Oteyza et al. 2004) suggests that the combined activities of the cyanobacteria and the associated organotrophic microorganisms are crucial for the degradation of hydrocarbons. Cyanobacteria may be important for emulsification of the oil, thereby facilitating further degradation (Cohen 2002).

A previous study showed that petroleum model compounds, immobilized on modified, hydrophobic clay and added on top of a pristine hypersaline microbial mat, decreased in the mat over time without significant changes of metabolic activity and microbial community composition (Grötschel et al. 2002). This study also showed that the added petroleum compounds remained mainly in the top layer of the mat and that the compounds were degraded by the pristine mat at low rates, with aromatic compounds being degraded faster than aliphatics. Our study, where a rapid decrease of *n*-alkanes (Fig. 8) occurred together with an increase of aerobic heterotrophic activity (Figs. 3, 4), suggests that in crude oil, which is a complex mixture of different classes of chemical compounds, some constituents stimulate/support the degradation process. We also observed a lower decrease of photosynthetic activity in the contaminated mats at the end of the experiment as compared to the control mat. Besides a direct stimulating effect of the (additional) CO_2 evolving from aerobic respiration of the hydrocarbons on photosynthesis, nitrogen-rich compounds in the oil could have led to the relative increase of photosynthesis in the contaminated mats. The sulphur-rich oil applied in this study is also nitrogen-rich and contains ~0.5% nitrogen, partly in the form of carbazoles. The carbazoles present in the crude oil are degraded by co-cultures of *Microcoleus* consortia, consisting of the mat-building *Microcoleus* and heterotrophic bacteria in their polysaccharide sheath (García de Oteyza et al. 2004). Thus, the nitrogen-rich compounds in the oil could help the cyanobacteria to overcome a potential nitrogen limitation, leading to an increase of photosynthesis. However, the precise role of these compounds on the activity of the mat and on oil degradation by mats remains to be investigated in detail.

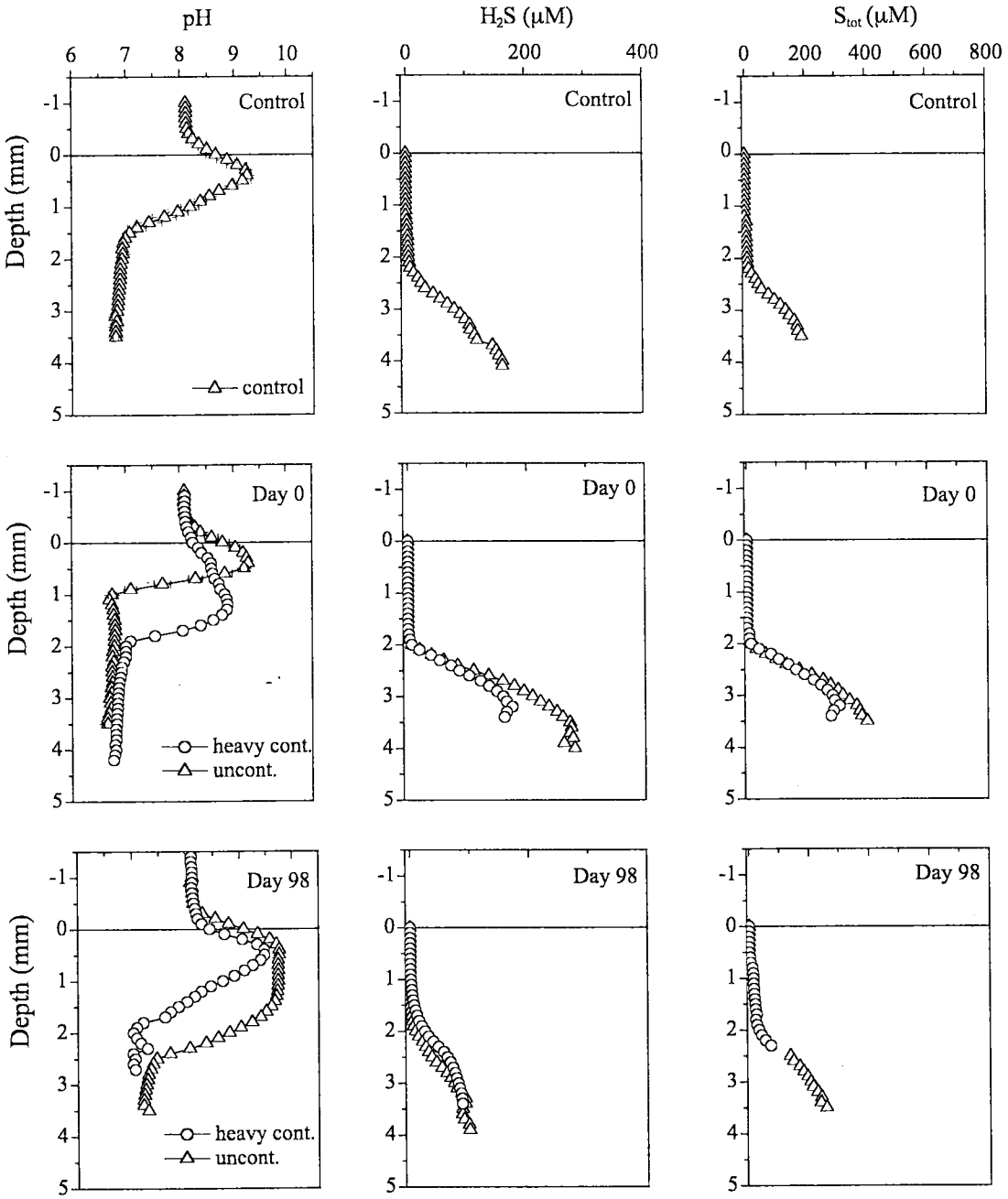

Fig. 6. Average steady-state concentration profiles (n = 2-3) of pH, H_2S, and S_{tot} as a function of time in the illuminated mats (348 μmol photons m^{-2} s^{-1}).

In response to oil contamination the production of exopolymers by the mat increased macroscopically (Fig. 1). Microbial exopolysaccharides seem to play a role in microbial oil degradation via their excellent oil-emulsifying properties (Bouchotroch et al. 2000, Iwabuchi et al. 2002). This could reduce the toxic effect of oil and make the hydrocarbons accessible for microbial biodegradation.

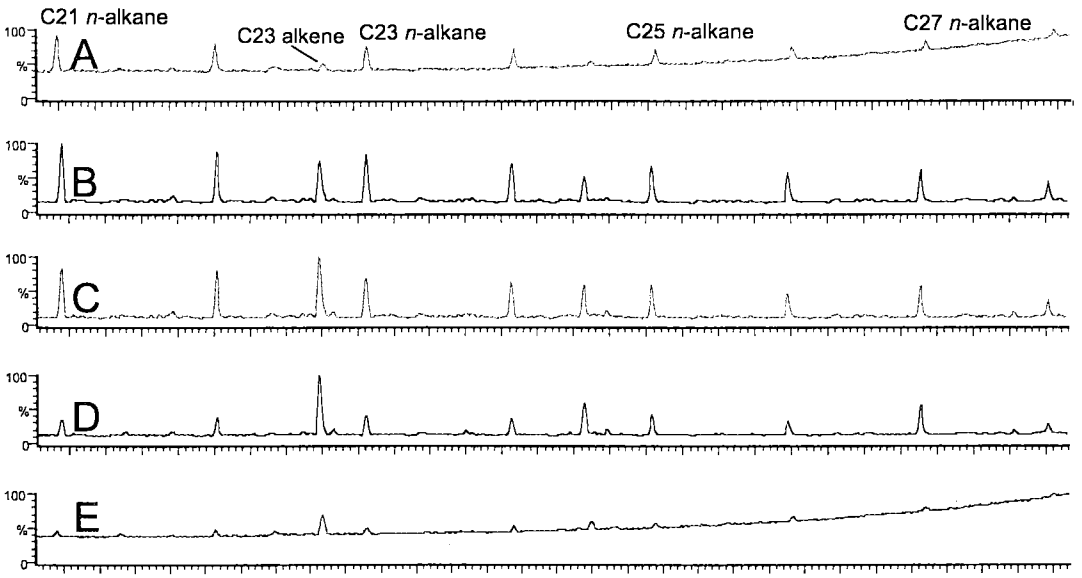

Fig. 7. Chromatogram of *n*-alkanes in the heavily contaminated mat at day 0 (A), day 7 (B), day 14 (C), day 26 (D), and day 98 (E), respectively. The unnamed peaks in the chromatogram are lipid biomarkers. Quantification of *n*-alkanes was relative to a microbial mat lipid, *n*-triacos-1-ene.

CONCLUSIONS

A general decrease of photosynthesis rates, O_2 concentrations, sulphide turnover rates and total sulphide concentrations in the uncontaminated mat was observed over time, suggesting a decrease of the overall activity of the mat, most probably caused by substrate/nutrient limitation. In mats contaminated with different amounts of sulphur-rich crude oil, a stimulation of O_2-consuming processes, as compared to the control was found. Microsensor measurements in the heavily contaminated mat showed that total sulphide concentrations and thus sulphate reduction rates decreased over time. Thus effects on O_2 consumption were therefore most probably not caused by increased sulphide oxidation, but due to an increase of heterotrophic aerobic respiration in the oil-contaminated mats. Gas chromatography of subsamples showed that $C_{21\text{-}28}$ alkanes from the added crude oil were degraded/oxidized over time within the mat, indicating aerobic biodegradation of these alkanes in the mat. Exopolysaccharides produced by the mat-inhabiting microorganisms in response to oil contamination could have increased the bioavailability of hydrocarbons for microbial degradation. Thus, in line with a recent review (Cohen 2002) we conclude that hypersaline microbial mats seem to possess a high potential for degradation of crude oil and possibly also other environmental pollutants (e.g., heavy metals, pesticides, etc.).

MATERIAL AND METHODS

Sampling

A microbial mat sample (30 x 20 cm) was taken at the sampling site located in Salin-de-Giraud (Camargue, France). A detailed description of the sampling site is given in Caumette et al. (1994), of the microbial community composition in Fourçans et al. (2004), and of the mat biogeochemistry in Wieland et al. (2004). *In situ* temperature and salinity were 20°C and ~90‰ at the time of sampling. Mat samples were transported within 6h to the Marine Biological Laboratory, University of Copenhagen, Helsingør, Denmark, and maintained for several days under *in situ*-like conditions (see below). Control microsensor measurements were performed in the mat before contamination with crude oil.

Contamination

The microbial mat sample was cut into 3 pieces of equal size and surface topography (8 x 17 x 3 cm) and placed in 3 glass aquaria (10 l) with-

out water. Two of the mat subsamples were contaminated with different amounts (8.23 and 16.46 ml/100 cm^2) of a viscous and sulphur-rich (>2% sulphur) crude oil (Maya oil), originating from evaporitic source rocks (for details on Maya oil composition see García de Oteyza & Grimalt, this issue). Sulphur-rich oils are increasingly used for the production of fuel products, but represent a high environmental risk due to their persistence in the environment after spillage.

Equal amounts of oil (7 ml) were dispersed homogeneously over both mat surfaces. The mats were kept dark and moist for 18 h to allow sufficient oil penetration into the mats. Thereafter, one mat piece was again contaminated with the same amount of oil and incubated under the same conditions (heavily contaminated mat). After another 48 h and a total incubation time of 66 h, artificial seawater was added to the contaminated mats. The oil fraction leaving the mat into the water was removed with filter paper.

The third mat piece, i.e., the control mat, was kept under the same conditions (dark and moist) during the contamination period of the other two mats. The three mat samples were placed in the microcosms and microsensor measurements were performed in all three mats 0, 6, 13, 26, and 98 days after the contamination.

Microcosms

The microbial mat samples were kept under identical conditions in the 3 glass aquaria with aerated artificial seawater (90‰). Water mixing and flow was generated with submersible water pumps (Power Head, Italy). The aquaria were placed side-by-side and illuminated with 3 x 500W and 10 x 20W halogen light sources. A light cycle of 4 stages was applied: 1 h 1500W, 2 h 1600W, 4 h 1700W, 2 h 1600W and 15 h darkness. The maximal downwelling scalar irradiance at the mat surface was quantified with a light meter (Biospherical Instruments, USA) and amounted to 700 µmol photons m^{-2} s^{-1}. The microcosms were kept in a cooling room (15°C) with additional cooling provided by 2 electric fans. The water temperature varied between 15°C (dark) and 30°C (maximal light) depending on the irradiance. Similar temperature fluctuations were observed at the field site. Mat subsamples (5 x 3 cm) were taken frequently from the microcosms and microsensor measurements were conducted (see below). After microsensor measurements, each subsample was frozen in liquid N_2 for further analyses.

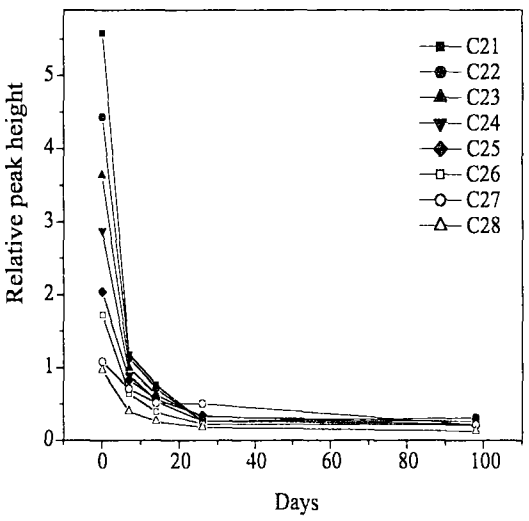

Fig. 8. Relative content of C_{21}-C_{28} alkanes in the heavily contaminated mat over time.

Microsensors

Clark-type O_2 (Revsbech 1989) and H_2S (Jeroschewski et al. 1996, Kühl et al. 1998) microsensors, and glass pH microelectrodes (Revsbech & Jørgensen 1986) were used to measure the distribution of oxygen and sulphide in the microbial mat. The O_2 microsensors had tip diameters of <10 µm, a stirring sensitivity of <2% and a t_{90} response time of <0.5 s. The H_2S microsensors, which were coated with black paint to avoid light interference on the measuring signal (Kühl et al. 1998), had tip diameters of <20 µm. The length of the pH-sensitive glass tip of the pH microelectrode was ~100 µm, with a tip diameter of ~15µm. The O_2 and pH microsensors were calibrated according to Wieland et al. (2003). The H_2S microsensors were calibrated according to Wieland et al. (2004). Total sulphide concentration, S_{tot}, in the mat was calculated from H_2S and pH microprofiles according to Wieland & Kühl (2000b).

The pH and H_2S microsensors were glued together after orienting the microsensor tips as close as possible to each other in the same horizontal plane. Oxygen, pH, and H_2S measurements were done subsequently with a motorized micromanipulator (Märzhäuser, Germany; MICOS GmbH, Germany; Jenny Electronics AG, Switzerland) mounted on a heavy solid stand. Microsensor signals were recorded with

a strip chart recorder (Kipp&Zonen, Netherlands) and with a computer data acquisition system (Profix, Unisense A/S, Denmark) that also controlled the micromanipulator. Experimental light-dark shifts for gross photosynthesis measurements were realized by manually darkening the mat surface. The moment of darkening was registered by a photodiode positioned in the light beam. The initial rate of O_2 depletion after darkening was calculated and stored by the software (Sloper, Unisense A/S, Denmark), and was used for calculation of gross photosynthesis rates (Kühl et al. 1996, Revsbech & Jørgensen 1983).

Microsensor set-up

For microsensor measurements, mat subsamples were embedded in agar (1.5% w/v) and mounted in a flow chamber (Lorenzen et al. 1995). A constant flow of aerated artificial seawater (90 ‰) was generated with a submersible water pump (Aqua Clear, Germany) connected to the flow chamber. The mat samples were illuminated with a fiber-optic halogen light source (KL 2500, Schott, Germany). The downwelling scalar irradiance at the mat surface was quantified as described above and amounted to 348 μmol photons m^{-2} s^{-1}. This moderate light intensity, in comparison to the microcosms, was chosen as higher irradiances led to intense bubble formation in the mat.

Calculations

Fluxes of O_2 across the mat-water interface were calculated according to Fick's first law of diffusion:

$$J_0 = -D_0 \, dC/dz \qquad (1)$$

where D_0 represents the molecular diffusion coefficient of O_2 in water and dC/dz is the concentration gradient in the diffusive boundery layer (DBL). The D_0 of O_2 was taken from Broecker & Peng (1974) and calculated as a function of temperature and salinity after Li & Gregory (1974). The concentration gradient was estimated from the linear part of the O_2 profile in the DBL (Jørgensen & Revsbech 1985). In darkness, J_0 represents dark O_2 consumption rates of the mat, R_{dark}, whereas in light it is a measure of net photosynthesis rates. The thickness of the effective DBL, δ_e, was calculated by extrapolation of the linear concentration gradient of O_2 in the DBL to the O_2 concentration in the water column after Jørgensen & Revsbech (1985).

The downward O_2 flux into the mat, J_s, was calculated from O_2 microsensor profiles by

$$J_s = -\phi D_s \, dC/dz \qquad (2)$$

where ϕ is the mat porosity and D_s is the sediment diffusion coefficient. The mat porosity was assumed to equal 0.9 and the mat diffusion coefficient D_s was calculated according to Ullman & Aller (1982).

Areal rates of gross photosynthesis (P_g) were calculated by depth-integration of the porosity-corrected volumetric gross photosynthesis rates in the zone where photosynthesis was measurable with the light-dark shift method (photic zone).

Chemical analyses

To determine the content of oil compounds in the mat after contamination and during the degradation experiment, the uppermost ~0.1-0.3 cm of the frozen mat samples (taken and frozen after the microsensor measurements) were extracted and analysed by gas chromatography.

For this, the samples were ground in a mortar and extracted twice with methanol (Merck), dichloromethane (Merck) and *n*-hexane (Merck) for 10 min in an ultrasonic bath. The total extract was fractionated by column chromatography in a 34 cm x 0.9 cm (i.d.) column filled with 8 g of both 5% water-deactivated alumina (top) and silica (bottom). The latter were prepared by extracting neutral silica gel (70-230 mesh, Merck) and alumina (70-230 mesh, Merck) with (2:1, v/v) dichloromethane-methanol in a Soxhlet apparatus for 24 h. After solvent evaporation, the silica and alumina were heated for 12 h at 120°C and 350°C, respectively. Finally, 5% of Milli-Q-grade water was added to these adsorbents for deactivation.

From the total extract of the mat samples, the aliphatic hydrocarbons were separated by elution with 20 ml of *n*-hexane, the monocyclic aromatic hydrocarbons (crude oil) and alkenes (microbial mat) were eluted with 10% dichloromenthane in *n*-hexane, and the polycyclic aromatic hydrocarbons (crude oil) with 20% dichloromenthane in *n*-hexane, respectively. As only typical petroleum components were of interest, further fractions, including two resin fractions (crude oil) with alkenones and sterols originating from the mat, were not analyzed. The hydrocarbon fractions were evaporated to dryness and redissolved in *iso*-octane.

Gas chromatography (GC) was performed

with a Varian Model Star 3400 equipped with a flame ionization detector and a Varian 8200 CX injector. A DB-5 capillary column (30 m x 0.25 mm i.d.; film thickness 0.25 mm) was used with hydrogen as carrier gas (50 cm/s). The oven temperature program was 70 to 140°C at 10°C/min, 140 to 310°C at 4°C/min (holding time 20 min). Injector temperature program was 100 to 300°C at 200°C/min and the detector temperature was 330°C (SPI Injection). Nitrogen was used as make up gas (30 mL/ min), whereas detector gas flows were hydrogen (30 mL/min) and air (300 mL/min).

Samples were also analyzed on a GC coupled to a mass spectrometer (GC-MS; Fisons MD-800). Spectra were obtained in the electron impact mode (70 eV) scanning from mass 50 to 550 every second. A HP-5 capillary column (30 m x 0.25 mm i.d.; film thickness 0.25 mm) was used with helium as carrier gas (1 ml/min). The oven temperature program was 70 to 140°C at 10°C/min, 140 to 310°C at 4°C/min (holding time 20 min). Injector, transfer line and ion source temperatures were 300, 280 and 200°C, respectively. Injection was in the splitless mode (*iso*-octane, hot needle technique) keeping the split valve closed for 48 s.

ACKNOWLEDGEMENTS

This study was supported by the European Commission (MATBIOPOL, EVK3-CT-1999-00010) and the Danish Natural Science Research Council. We thank the salt company Salins-du-Midi, Salin-de-Giraud, France for providing access to the field site. Anni Glud is gratefully acknowledged for construction of microsensors and technical assistance.

REFERENCES

Al Hasan RH, Sorkoh NA, Al Bader D & Radwan SS (1994) Utilization of hydrocarbons by cyanobacteria from microbial mats on oily costs of the Gulf. - *Applied Microbiology and Biotechnology* **41**: 615-619.

Atlas RM & Bartha R (1992) Hydrocarbon biodegradation and oil spill bioremediation. - *Advances in Microbial Ecology* **12**: 287-338.

Bartha R & Atlas RM (1977) The microbiology of aquatic oil spills. - *Advances in Applied Microbiology* **22**: 225-266.

Bertrand JC, Caumette P, Mille G, Gilewicz M & Denis M (1989) Anaerobic biodegradation of hydrocarbons. - *Sci Prog* **73**: 333-350.

Bouchotroch S, Quesada E, Izquierdo I, Rodríguez M & Béjar V (2000) Bacterial exopolysaccharides produced by newly discovered bacteria belonging to the genus *Halomonas*, isolated from hypersaline habitats in Morocco. - *J Ind Microbiol Biotechnol* **24**: 374-378.

Broecker WS & Peng T-H (1974) Gas exchange rates between air and sea. - *Tellus* **26**: 21-35.

Canfield DE & Des Marais DJ (1993) Biogeochemical cycles of carbon, sulfur, and free oxygen in a microbial mat. *Geochimica et Cosmochimica Acta* **57**: 3971-3984.

Caumette P, Matheron R, Raymond N & Relexans J-C (1994) Microbial mats in the hypersaline ponds of Mediterranean salterns (Salins-de-Giraud, France). - *FEMS Microbiology Ecology* **13**: 273-286.

Cerniglia C, Van Balen C & Gibson DT (1980) Oxidation of biphenyl by the cyanobacterium *Oscillatoria* sp. strain JCM. - *Archives of Microbiology* **125**: 203-207.

Cohen Y (1989) Photosynthesis in cyanobacterial mats and its relation to the sulfur cycle: a model for microbial sulfur interactions. - In: Cohen Y & Rosenberg E (eds) *Microbial mats: Physiological ecology of benthic microbial communities*, American Society for Microbiology: pp. 22-36.

Cohen Y (2002) Bioremediation of oil by marine microbial mats. *International Microbiology* 5: 189-193.

Cornée A, Dickman M & Busson G (1992) Laminated cyanobacterial mats in sediments of solar salt works: some sedimentological implications. - *Sedimentology* **39**: 599-612.

Ellis BE (1977) Degradation of phenolic compounds by freshwater algae. - *Plant Science Letters* **8**: 213-216.

Epping E & Kühl M (2000) The responses of photosynthesis and oxygen consumption to short-term changes in temperature and irradiance in a cyanobacterial mat (Ebro Delta, Spain). - *Environmental Microbiology* **2**: 465-474.

Fingas M (2001). The basics of oil spill cleanup, Lewis Publishers.

Fourçans A, García de Oteyza T, Wieland A, Solé A, Diestra E, van Bleijswijk J, Grimalt JO, Kühl M, Esteve I, Muyzer G, Caumette P & Duran R (2004) Characterization of functional groups in a hypersaline microbial mat community (Salins-de-Giraud, Camargue, France). - *FEMS Microbiology Ecology*: in press.

García de Oteyza T & Grimalt JO (2004) Molecular composition of the gas chromatography amenable fractions of Maya crude oil. A reference oil for microbial degradation experiments. - *Ophelia* (this issue): submitted.

García de Oteyza T, Grimalt JO, Diestra E, Solé A & Esteve I (2004) Changes in the composition of polar and apolar crude oil fractions under the action of *Microcoleus* consortia. - *Applied Microbiology Biotechnology*: in press.

Glud RN, Ramsing NB & Revsbech NP (1992) Photosynthesis and photosynthesis-coupled respiration in natural biofilms quantified with oxygen microsensors. - *Journal of Phycology* **28**: 51-60.

Grötschel S, Köster J, Abed RMM & de Beer D (2002) Degradation of petroleum model compounds immobilized on clay by a hypersaline microbial mat. - *Biodegradation* **13**: 273-283.

Hoffmann L (1996) Recolonisation of the intertidal flats by microbial mats after the Gulf War oil spill. - In: Krupp F, Abuzinada AH & Nader IA (eds) *A marine wildlife sanctuary for the Arabian Gulf*, Senckenbergische Naturforschende Gesellschaft: 96-115.

Holliger C, Gaspard S, Glod G, Heijman C, Schumacher W, Schwarzenbach RP & Vazquez F (1997) Contaminated environments in the subsurface and bioremediation: organic contaminants. - *FEMS Microbiology Reviews* **20**: 517-523.

Iwabuchi N, Sunairi M, Urai M, Itoh C, Anzai H, Nakajima M & Harayama S (2002) Extracellular polysaccharides of *Rhodococcus rhodochrous* S-2 stimulate the degradation of aromatic components in crude oil by indigenous marine bacteria. - *Applied and Environmental Microbiology* **68**: 2337-2343.

Javor BJ (1989) *Hypersaline environments, Springer.*

Jeroschewski P, Steuckart C & Kühl M (1996) An amperometric microsensor for the determination of H_2S in aquatic environments. - *Analytical Chemistry* **68**: 4351-4357.

Jørgensen BB (1994) Diffusion processes and boundary layers in microbial mats. - In: Stal L & Caumette P (eds) *Microbial Mats: Structure, Development and Environmental Significance, NATO ASI Series, Springer.* 243-253.

Jørgensen BB (2001) Life in the diffusive boundary layer. - In: Boudreau BP & Jørgensen BB (eds) *The benthic boundary layer: Transport processes and biogeochemistry, Oxford University Press*: 348-373.

Jørgensen BB & Des Marais DJ (1990) The diffusive boundary layer of sediments: oxygen microgradients over a microbial mat. -*Limnology & Oceanography* **35**: 1343-1355.

Jørgensen BB, Nelson DC & Ward D M (1992) Chemotrophy and decomposition in modern microbial mats. - In: Schopf J & Klein C (eds) *The proterozoic biosphere: a multidisciplinary study, Cambridge University Press*: 287-293.

Jørgensen BB & Revsbech NP (1985) Diffusive boundary layers and the oxygen uptake of sediments and detritus. - *Limnology & Oceanography* **30**: 111-122.

Kivaisi AK (2001) The potential for constructed wetlands for wastewater treatment and reuse in developing countries: a review. - *Ecological Engineering* **16**: 545-560.

Kühl M, Glud RN, Ploug H & Ramsing NB (1996) Microenvironmental control of photosynthesis and photosynthesis-coupled respiration in an epilithic cyanobacterial biofilm. - *Journal of Phycology* **32**: 799-812.

Kühl M & Jørgensen BB (1992) Microsensor measurements of sulfate reduction and sulfide oxidation in compact microbial communities of aerobic biofilms. - *Applied and Environmental Microbiology* **58**: 1164-1174.

Kühl M, Steuckart C, Eickert G & Jeroschewski P (1998) A H_2S microsensor for profiling biofilms and sediments: application in an acidic lake sediment. - *Aquatic Microbial Ecology* **15**: 201-209.

Kühl, M., Fenchel, T., and Kazmierczak, J. (2003) Growth, structure and calcification potential of an artificial cyanobacterial mat. In: Krumbein, W.E., Paterson D., and Zavarzin G. (eds.), *Fossil and recent biofilms, a natural history of life on Earth.* Kluwer Acad. Publ., Dordrecht pp. 77-102.

Kuo L-C 1994 An experimental study of crude oil alteration in reservoir rocks by water washing. - *Organic Geochemistry* **21**: 465-479.

Li Y-H & Gregory S (1974) Diffusion of ions in sea water and in deep-sea sediments. - *Geochimica et Cosmochimica Acta* **38**: 703-714.

Lorenzen J, Glud RN & Revsbech NP (1995) Impact of microsensor-caused changes in diffusive boundary layer thickness on O_2 profiles and photosynthetic rates in benthic communities of microorganisms. - *Marine Ecology Progress Series* **119**: 237-241.

Mashauri DA, Mulungu DMM & Abdulhussein BS (2000) Constructed wetland at the university of Dar Es Salaam. - *Water Research* **34**: 1135-1144.

Narro ML (1985) Petroleum toxicity and the oxidation of aromatic hydrocarbons. - In: Fay P & Van Baalen C (eds) *The Cyanobacteria, Elsevier.* 493-511.

Obuekwe CO & Al-Zarban SS (1998) Bioremediation of crude oil pollution in the kuwait desert: the role of edherent microorganisms. - *Environmental International* **24**: 823-834.

Revsbech NP (1989) An oxygen microelectrode with a guard cathode. - *Limnology & Oceanography* **34**: 474-478.

Revsbech NP & Jørgensen BB (1983) Photosynthesis of benthic microflora measured with high spatial resolution by the oxygen microprofile method: Capabilities and limitations of the method.- *Limnology & Oceanography* **28**: 749-756.

Revsbech NP & Jørgensen BB (1986) Microelectrodes: Their use in microbial ecology. - *Advances in Microbial Ecology* **9**: 293-352.

Shutes RBE, Revitt DM, Lagerberg IM & Barraud VCE (1999) The design of vegetative constructed wetlands for the treatment of highway runoff. - *The Science of the Total Environment* **235**: 189-197.

Sorkhoh N, Al-Hasan R & Radwan S (1992) Self-cleaning of the Gulf. - *Nature* **359**: 109.

Ullman WJ & Aller RC (1982) Diffusion coefficients in nearshore marine sediments. - *Limnology & Oceanography* **27**: 552-556.

Wieland A & Kühl M (2000a) Irradiance and temperature regulation of oxygenic photosynthesis and O_2 consumption in a hypersaline cyanobacterial mat (Solar Lake, Egypt). - *Marine Biology* **137**: 71-85.

Wieland A & Kühl M (2000b) Short-term temperature effects on oxygen and sulfide cycling in a hypersaline cyanobacterial mat (Solar Lake, Egypt). - *Marine Ecology Progress Series* **196**: 87-102.

Wieland A, Kühl M, McGowan L, Fourçans A, Duran R, Caumette P, García de Oteyza T, Grimalt JO, Solé A, Diestra E, Esteve I, Herbert RA (2003) Microbial mats on the Orkney Islands revisited: microenvironment and microbial community composition. - *Microbial Ecology* **46**: 371-390.

Wieland A, Zopfi J, Benthien M and Kühl M (2004) Biogeochemistry of an iron-rich hypersaline microbial mat (Camargue, France). - *Microbial Ecology*: in press.